We are IntechOpen,
the world's leading publisher of
Open Access books
Built by scientists, for scientists

6,900
Open access books available

186,000
International authors and editors

200M
Downloads

Our authors are among the

154
Countries delivered to

TOP 1%
most cited scientists

12.2%
Contributors from top 500 universities

CLARIVATE ANALYTICS

BOOK CITATION INDEX

INDEXED

WEB OF SCIENCE™

Selection of our books indexed in the Book Citation Index
in Web of Science™ Core Collection (BKCI)

Interested in publishing with us?
Contact book.department@intechopen.com

Photoluminescence in Doped PZT Ferroelectric Ceramic System

M. D. Durruthy-Rodríguez[1] and J. M. Yáñez-Limón[2]
[1]Cybernetic, Mathematics and Physics Institute
[2]Centro de Investigación y de Estudios Avanzados del Instituto Politécnico Nacional
[1]Cuba
[2]Mexico

1. Introduction

The photoluminescence (PL) it is a non thermal origin process, in that a chemical compound absorbs the photons (of the electromagnetic radiation), jumping to an electronic state of more energy, the inverse process happens and so call recombination (when passing to inferior energy level) and the materials radiating photons. The period between absorption and emission occur is in order to 10 nanoseconds. But under special circumstances, this period can extend in minutes or hours. The transition energy is determined by quantum mechanics rules. Different imperfection presents in the materials study will alter the recombination time or frequency.

Simpler PL processes are resonant radiations, in that a photon of a particular longitude wave is absorbed and an equivalent photon is emitted immediately. This process doesn't involve any transition in forbidden energy band and it is extremely quick (10 ns). The most interesting processes happen when the desexcitation energy transition is not direct at the basic level. The most common effect is the fluorescence that is also typically a quick process, but in that the original energy it is dissipated so that the slight photons emitted are of the lower energy that those absorbed. This phenomenon can happen for the isolated atoms, molecules or atoms and molecules in interaction excitement.

1.1 Atomic, molecular and atoms and molecules in interaction luminescence

The isolated atom excitement (making notice that a very rarefied gas can be considered as a group of isolated atoms) it drives to a spectrum of lines. The atom only absorb the frequency of the incident ray that corresponds to the allowed transitions (Figure 1). So all the isolated atoms can be luminescent.

That happens for the isolated atoms is also valid for the isolated molecules, but the laws are more complicated due to the vibrations and rotations molecular than they introduce supplementary energy levels as the sample the following diagram of figure 2.

The pressure of a gas it increases and a new transitions of excitement energy appear by collision, for the appearance of kinetic energy and metastable states. The return to the basic state is with a reduction of the yield of the luminescence and an expansion of the spectrum of the transmission. Then appears spectrum of band. The return to the fundamental state it doesn't always happen with light emission (transitions without radiation).
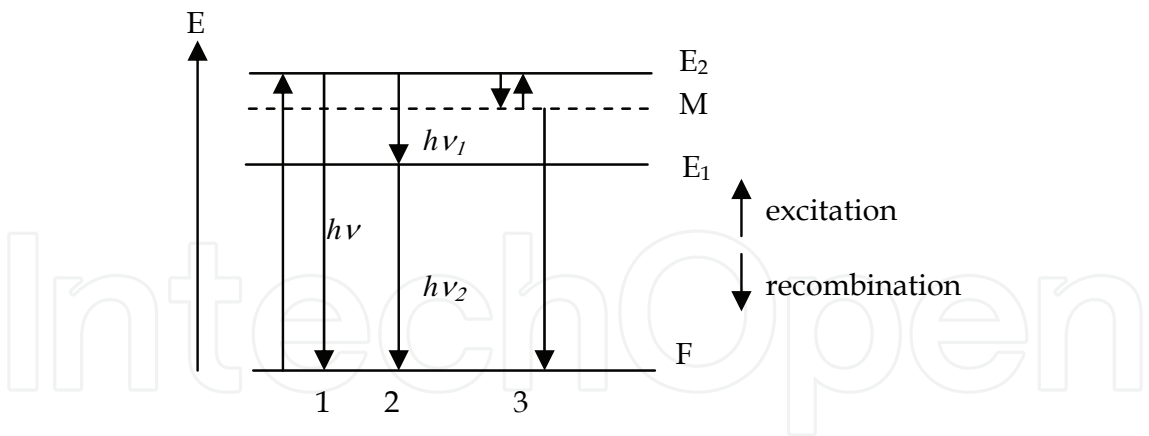
Fig. 1. Three possible luminiscence types of an isolated atom:

1) direct transition, this is a resonance phenomenon;

2) indirect transition, distributing the energy in several photons hv_1 and hv_2 ,

3) indirect transition by a metastable state (M) following by interatomic collision (not very probable).

1.2 Crystalline luminescence

The luminescence of the crystalline bodies is due to the transmission centers (the activators). These centers are:

-   physical imperfections in crystalline structure (vacancies, interstitial atoms, dislocations), this is intrinsic luminiscence.
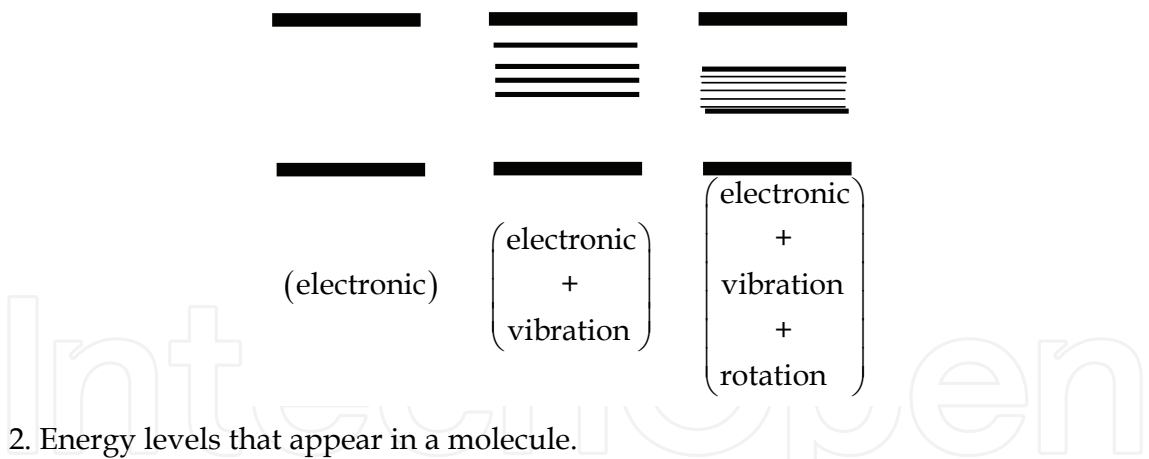

Fig. 2. Energy levels that appear in a molecule.

-   chemical imperfections (impurity atoms) in interstitial or substitution position, this is extrinsic luminiscence.

The mechanism of crystalline luminiscence it is explained with the help of energy bands diagram (Figure 3).

Considering that in the perfect crystal any level doesn't exist in forbidden band, the presence of imperfection in the cystal introduces some levels allowed in the forbidden or in the allowed bands. These energy levels they can be:

-   recombinations levels (h/e -)

-   metastable levels: the traps of e- (Pe) or h (Pt)

-   fundamental (F) and excited levels (E) of isolated centers

The spectra of crystalline luminiscence differ notably of the atomic spectra for two fundamental aspects. 1): bands are observed and 2) the emitted radiation appears toward the longitude of big waves, this can made a mistake with the absorbed radiation. These two aspects are due to the interaction between the emission center and the crystalline lattice.

According to the type of imperfections there are the transitions way and therefore the energy of the transition.

A first transition consists on an electron that leaves a donor level and go toward the valency band. The energy of this transition is given for: E=Egap-Ed

Also, can be observed where an electron leaves to the conduction band to pass at aceptor level. In this case, the energy of the transition is given for: E=Egap-EA
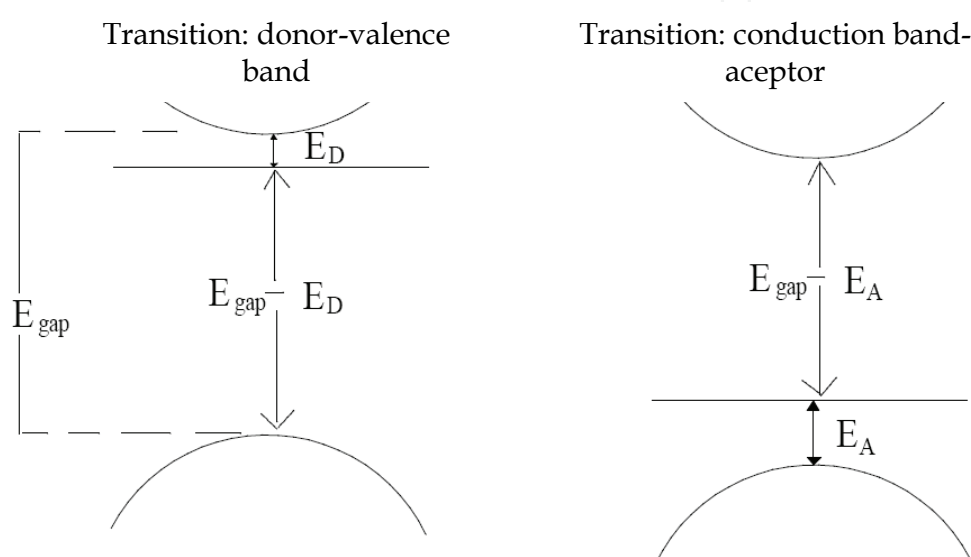

Fig. 3. Types of transitions among bands.

It is known that the energy E_D and E_A differ according to the chemical nature of the impurity. For this reason is allows to use the photoluminiscence experiments to confirm the presence of a specific type of impurity in a material.

In many cases, the theory of the effective mass is a first valid approach, it predicts the value of the energy E_D and E_A for a given semiconductor.

$$E_D = \frac{13.6eV}{\varepsilon^2}\frac{m_e^*}{m_0} \quad \text{and} \quad E_A = \frac{13.6eV}{\varepsilon^2}\frac{m_h^*}{m_0} \tag{1}$$

In general $m_h^* \gg m_e^*$, it is explained, why the bond energy of aceptor levels is bigger than that donors levels.

Broad bands are observed for many optical transitions in the partly filled d-shell of transition metal ions (d - d transitions), but also for transitions between the 5d shell and the 4f shell of rare-earth ions (d - f transitions) and for emission on s^2 ions (these ions possess a ''lone pair'' of s electrons), like T^{1+}, Pb^{2+}, or Sb^{3+}. Sharp emission bands are characteristic of optical transitions between electronic states with chemical bonding character (almost) the same for ground and excited state, and for the same reason also of optical transitions between electronic states that hardly participate in the chemical bonding (e.g., f - f transitions on rare-earth ions).

In the case of optical processes involving electronic states which participate in the chemical bonding, the nature of the bonding (covalent, ionic) and the symmetry of the site at which the emitting ion is incorporated play a very important role. This is generally described by the ligand field theory, which we do not treat here.

The emission generated reflects how the optical properties of the ion depend on its chemical environment. This luminescent material can be applied as green phosphor in very high-quality fluorescent lamps and also in plasma display (Ronda, 2008).

2. Luminescence in PZT

The width of luminescent band usually observed at room temperatures in crystals of perovskite type it is associated with the presence of imperfections or defects (Haertling, 1999; Anicete-Santosaet al., 2007), be already oxygen or lead vacancies. But other author explain apparition of PL to order-disorder presence in the structure (Chen et al., 1989; Suárez-Gómez et al., 2009; Shannigrahi, 2007) distortion of oxygen octahedral fundamentally.

Undoped PZT ceramics are seldom used. They are usually substituted in the A or B-sites of the perovskite structure ABO_3 in order to improve dielectric, piezoelectric and mechanical properties. For example La^{3+} and Nb^{5+} are used satisfactorily (Durruthy et al., 1999, 2002; Bharadwaja et al., 2002). The excess of positive charge in (La/Nb) doped PZT is compensated by lead vacancies and the typical Kröger-Vink notation to describe the electroneutrality, have been reported in many papers previously (Eyraud et al, 2006; Jaffe et al., 1954).

The defects caused by the small dopant concentrations in A or B places of the structure could generate a combination of blue, green and red emission of light which is of great importance for optical devices applied in optoelectronics includes flat-screen, full-colour displays and compact laser devices operating in the blue region (Nakajima et al., 2004; Yang et al., 2008).

Recently M.S. Silva et. al., 2005, reported a theoretical and experimental result, and presents an alternative method to process PL in PZT and aim to explain why this phenomenon depends on the crystalline structure of the material. The wide bands at 2.1 and 2.67 eV respectively in PL emission in perovskite ceramics are associated to the oxygen vacancies provoked during the sintering process (Lines & Glass, 2001) or related to ensure electroneutrality process.

What happens with luminescence effect with A, B or A+B doped PZT?

We will try to respond this question with several examples.

All samples that show were prepared by a conventional processing method using mixed oxide powders. The photoluminescence (PL) spectra were obtained using a Jobin Yvon Horiba Fluoromax-3 spectrometer using the excitation band at 373 nm. The absorption spectra were acquired with an UV-vis Ocean Optics Spectrometer QE650000 using diffuse reflectance measurements the data was processed by using the Kubelka-Munk function:

$$F(R_\infty^{'}) = \frac{(1 - R_\infty^{'})^2}{2R_\infty^{'}} = \frac{a}{S} \tag{2}$$

$$R_\infty^{'} = \frac{R_\infty(sample)}{R_\infty(standard)} \tag{3}$$

$R_\infty = (I/I_0)$ is diffuse reflectance at one wavelength from an opaque sample with infinite thickness (> 2 μm), $0< R_\infty <1$, α is the absorbance in cm^{-1} and S is the scattering factor which is assumed to be independent of the wavelength for grain sizes greater than the wavelength of the light (Wendlandt & Hecht, 1966; Kottim, 1969).

Crystalline structure (Figure 4), like we will see later, influences in the shift energy of PL in the samples. For this reason it is advisable to carry out this study previously to PL analysis. All samples firth were identify by X-ray diffraction (XRD). The XRD patterns of the polycrystalline samples show the tetragonal (Zr/Ti = 20/80, 40/60) and rhombohedral (Zr/Ti = 60/40, 80/20) PZT phases, and both phase together for Zr/Ti = 53/47. This is a classical behavior for this material and has been reported by some authors (Jaffe et al., 1971; Noheda, 2000, 2001).

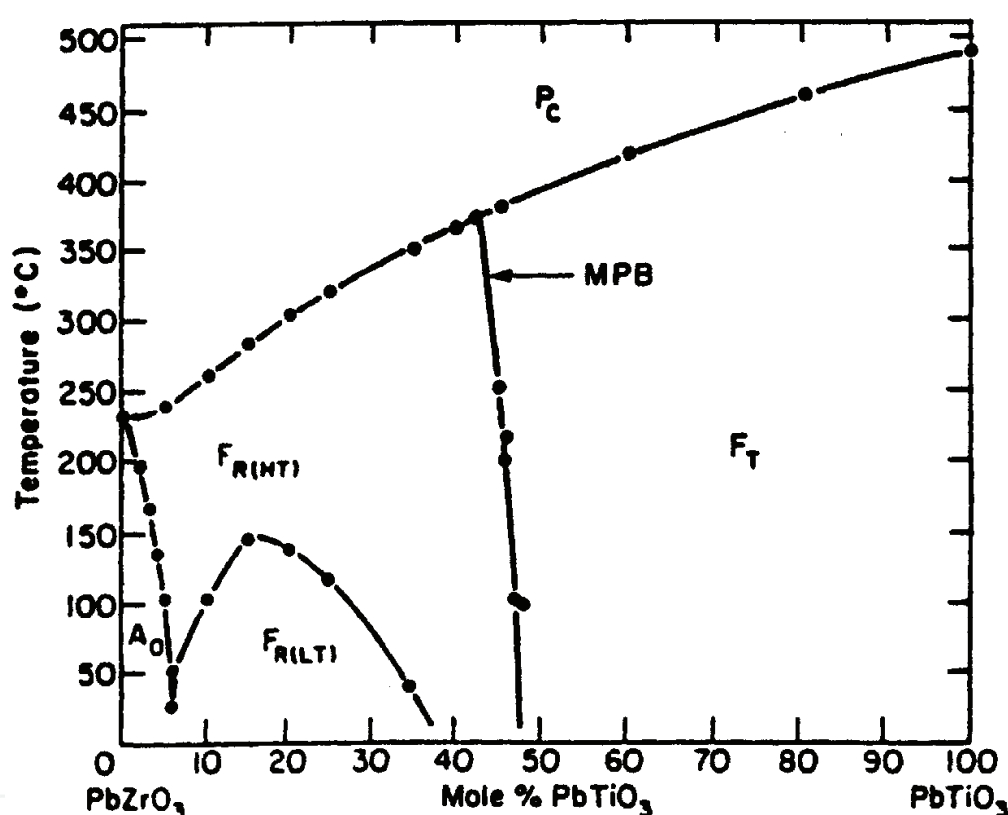
Fig. 4. Phases diagram of PZT, appear the existence range of each phase (tetragonal and rhombohedral), the morfotrópica phase boundary (MPB) according to Jaffe et al. (1971).

In our samples doped the compensation of charge provokes in all cases oxygen vacancies that should increase with the dopant concentration or saturates in a composition that denotes a limit of solubility. However, oxygen vacancies are easily induced during the sintering process because the PbO has low volatile temperature of about 880ºC. This phenomenon takes place in all samples and also promotes lead and oxygen vacancies, which are quenched defects at low temperatures. Lead vacancies can only become mobile at high temperatures with high activation energy greater than oxygen mechanism values.

According to Eyraud et. al. (2006) singly and doubly ionized lead and oxygen vacancies coexist in the PZT ceramic, then they may constitute donor and acceptor sites which are able to exchange electrons according to the following reactions:

$$V_{Pb} \rightarrow V_{Pb}' + e$$
$$V_{Pb}' \rightarrow V_{Pb}'' + e$$
$$V_O \rightarrow V_O^{\bullet} + e \qquad (4)$$
$$V_O^{\bullet} \rightarrow V_O^{\bullet\bullet} + e$$

in our case at least three types of defects coexist V_{Pb}', V_{Pb}'' and $V_O^{\bullet}$, whose contribution to PL depends on the levels in the band gap.

The results of first-principle calculation reported by Ghasemifard et al., (2009) show that the PZT polycrystalline has a direct band gap between the X and Γ points of 3.03 eV (Baedi et al., 2008), then by assuming a direct band gap we can calculate the values of the energy gap (Eg) for all the samples. In general calculating the absorption coefficients of the synthesized powder in the strong absorption region needs both, the transmission and reflection spectra. In our case, we obtained the absorption spectra by diffuse reflectance measurements, and by using the Kubelka-Munk equation for all samples the band gap energy Eg was determined.

2.1 Substitution in A site

The substitution for La³⁺ in the A site of perovskite structure it's traditional. It is one of the classic sustituyentes in this system.

The emission spectra (PL) at 273, 325, 373, 413 and 457 nm were characterized to present different bands for PLZT 1-x/x/y (Figure 5), prevailing blue-violet band presence (2.4-2.75 eV), it's appears at bigger intensity for 413 nm. This evidences that PL effect has the same origin in all cases.

As it has been expressed previously, the energy of the spectra of PL demonstrates the presence of levels in the forbidden band. The calculations of first principles (Longo et al., 2005) have been demonstrated that disorder in perovskite structure and the defects in the same one, they cause states in the forbidden band. On the other hand the experimental evidence of the presence of defects exists (oxygen vacancies) (Mansimenko et al., 1998) starting from mensurations of resonance electronic paramagnética (RPE) in the system PLZT.

If we consider to our materials as semiconductors of big gap, the presence of states in the forbidden band, what causes a contraction of the gap, is the causing of a well-known Burstein-Moss shift of emission spectrum (Yu & Cardona, 1996). It can associate to presence of picks around 2.65 eV to the presence of bands inside of forbiden band in the material, being more intensity when it's excited with λ= 413 nm.

Analyzing the results associating them with the colors corresponding of the wave longitudes, we see that emissions exist (although of different intensity) in almost the whole visible spectrum, from the red one until the ultra violet, but the bands of very high intensity correspond to the bands of the blue-violet and ultraviolet.

The motive that causes this effect are similar when you doped these materials in B site, this will be explained in the next section.

2.2 Substitution in B site

In perovskita structure (ABO₃) N⁵⁺ substitute B site, occupied by Zr⁴⁺ and Ti⁴⁺ ion. The high volatility of lead oxide at elevated temperatures during the powder calcinations and the
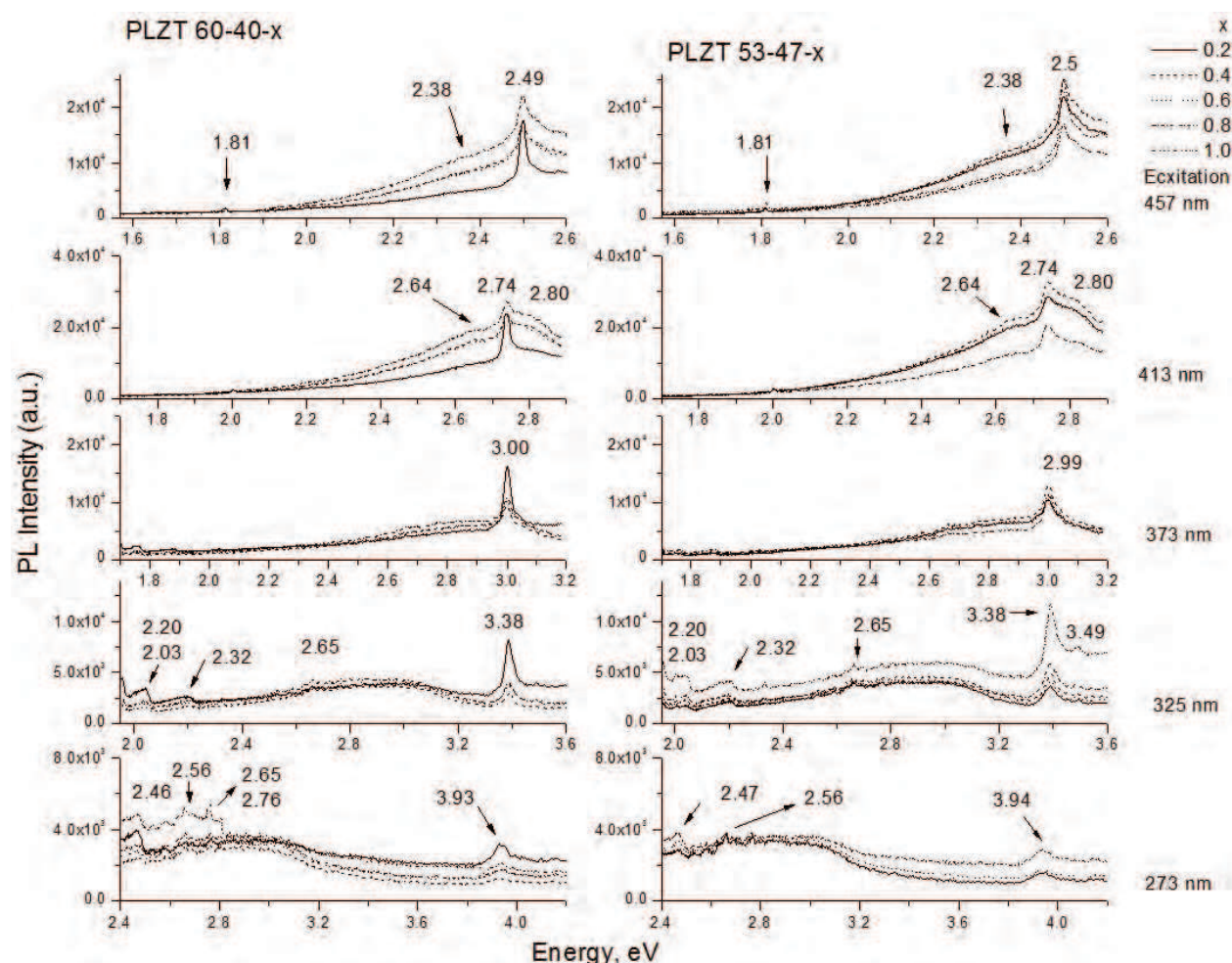
Fig. 5. PL spectra at room temperature, fixing the excitation band at 273, 325, 373, 413 and 457 nm in PLZT ferroelectric ceramics. Appear result for two point of PZT phase diagram doped at different La³⁺ concentration.

sintering stages in the PZT system is known, which provides both fully-ionized cationic lead $V_{Pb}^{''}$ vacancies and anionic oxygen vacancies $V_O^{\bullet\bullet}$. On the other hand, following Eyraud's model (Sivasubramanian et al., 2007; Chang et al., 2001) the valence of the Niobium is assumed as donor doping in the PZT has a strong influence in the ionization state of extrinsic lead and oxygen vacancies.

Figure 6 shows the PL spectra of PZTN samples for compositions 80/20, 60/40, 53/47, 40/60 and 20/80 which have diverse dopant concentrations. The emission bands (PL response) when fixing the excitation bands (EB) at 373, 457 and 325 nm were observed in three regions: one is at around 1.72 eV (lowest energy region); the second is at around 2.56 – 2.61 eV which shows a higher intensity, and the third is at around 3.35 – 3.45 eV (highest energy region) respectively. The band at 2.56 eV is the most intense and narrow, and the band at 3.35 eV shows greater broadening. The band at 1.72 eV did not show any notable shift in the maximum position peaks for different compositions or dopant concentrations. Nevertheless, the bands at 2.56 and 3.35 eV show a shift in the maximum peak position which depending if the phase is rhombohedral or tetragonal will shift to 2.61 and 3.45 eV, respectively.
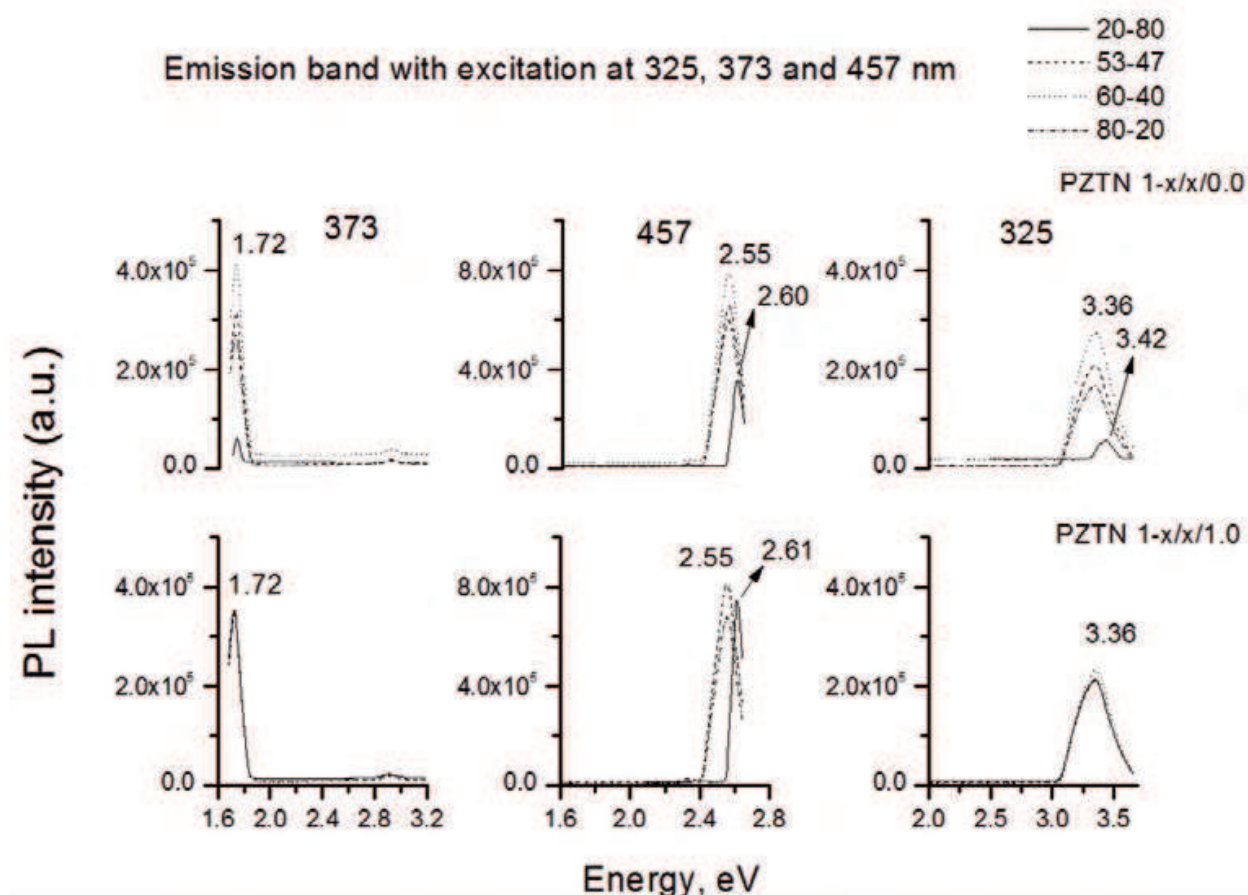
Fig. 6. Room temperature PL for PZTN note the dispersion for non doped materials. For PLZT 1-x/x/1.0 practically all the curves coincide for the same energy 1.72 and 3.36 for λ= 373 and 325 respectively.

Note that in the PZT polycrystalline samples without Nb, the three well resolved emission bands were also shown, in contrast with other reports (Longo et al., 2008; Chang et al., 2001) where the emission for polycrystalline PZT is very low and broad or absent. For these materials (PZTN) the emission is bigger in 1 or 2 order than PLZT. The PLE spectra for samples doped and without doped they present same character, appearing the same line, for what they have the same origin in both cases (Figure 7).

The E_g (in PZTN) values for tetragonal samples 20/80 and 40/60 are between 2.80 to 2.98 eV, the composition 53/47 are near the morphotropic phase boundary which shows a higher variation in E_g, values as a function of the dopant concentration from 2.70 to 3.19 eV. For this composition and rhombohedral phases 60/40 and 80/20 the behavior of E_g values as a function of Nb concentration shows a minimum at 0.8% with values of approximately 2.67 to 2.70 eV. In our case, experimentally it is observed a transition (E_{PL}) at 2.56 eV for samples PZTN 80/20/0.0.

Sintering stages in the PZT system is known, which provides both fully-ionized cationic lead V_{Pb}'' vacancies and anionic oxygen vacancies $V_O^{\bullet\bullet}$. On the other hand, following Eyraud's model (Sivasubramanian et al., 2007; Chang et al., 2001) the valence of the Niobium is assumed as donor doping in the PZT has a strong influence in the ionization state of extrinsic lead and oxygen vacancies.
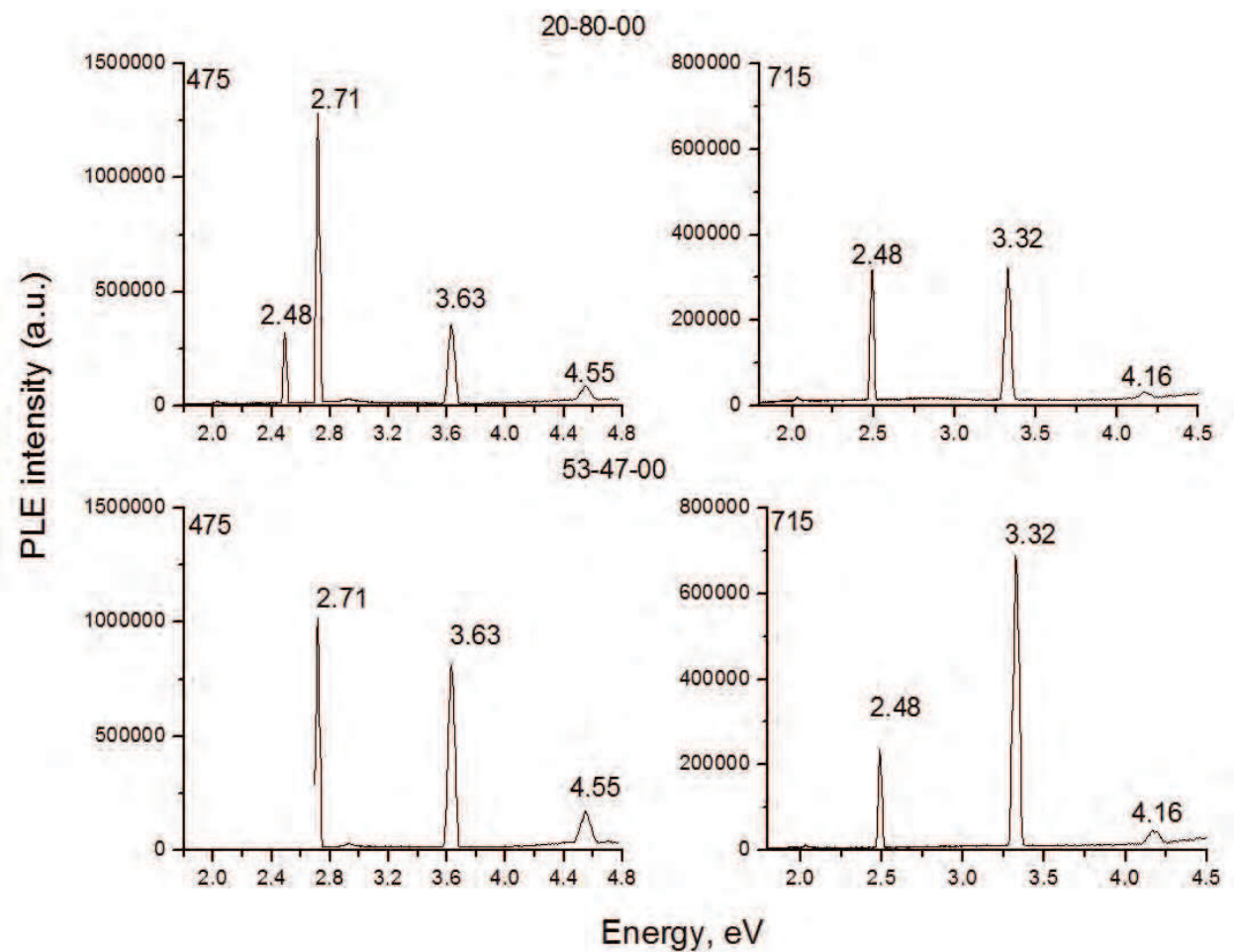
Fig. 7. Room temperature excitation spectra PLE for PZTN for an emission at 475 and 715 nm respectively.

The E_D values reported in Table 2 were calculated using E_g and E_{PL} obtained by excitation at EB=457 nm. Even the origins of these luminescence bands are not clearly understood. Figure 8 shows a schematic diagram to represent the recombination process for the three emission bands. The PL at a high energy region of approximately 3.35-3.45 eV, that overcomes the E_g, which is obtained when the excitation is at 3.81 eV.

% Nb	E_{gap} (Zr/Ti)									
	20/80		40/60		53/47		60/40		80/20	
	Eg	E_D	Eg	E_D	Eg	E_D	Eg	E_D	Eg	E_D
0.0	2.80	0.19	2.92	0.31	3.19	0.63	3.04	0.48	3.09	0.53
0.2	2.84	0.23	2.86	0.25	2.93	0.37	3.04	0.48	3.04	0.48
0.4	2.84	0.23	2.84	0.23	2.90	0.34	2.92	0.36	2.96	0.40
0.6	2.82	0.21	2.86	0.25	2.85	0.29	2.85	0.29	2.85	0.29
0.8	2.87	0.26	2.80	0.19	2.70	0.14	2.67	0.11	2.67	0.11
1.0	2.90	0.29	2.98	0.37	3.00	0.44	2.95	0.39	2.94	0.38

Table 1. Band gap energy (Eg) for PZTN, determined using the diffuse reflectance principle (Kubelka-Munk expression). Error Eg= ± 0.003 eV. ED values obtained with the Eg and more intense emission band at around 2.56 eV.

This corresponds to transitions between higher energy states in the conduction band to the valence band (hot luminescence), and the emission intensity shows a strong dependence on the Nb concentration.

The PL at 1.73 eV, the lowest energy region which is obtained with excitation energy of 3.32 eV, it could be follows a recombination mechanism:

1. from the localized states due to oxygen vacancies below the conduction band ($V_O^{\bullet}$) to the localized states above the valence band due to lead vacancies ($V_{Pb}^{'}$) and/or

2. by recombination from band conduction to the localized states above the valence band due to lead vacancies ($V_{Pb}^{''}$).

The intensity emission of this band also shows a strong dependence on Nb concentration, and is present in all compositions indicating common defect types related to a deep level inside the band gap. In general, the incorporation of Nb[5+] increases the PL intensity in this region due to the compensation of charge and induced defects ($V_{Pb}^{'}$ and $V_{Pb}^{''}$), as it was already seen previously.

In this case the simultaneous disorder of lead and oxygen vacancies should be created during the sintering process. The PL at 2.56 eV, which shows the highest intensity in all PZTN compositions and is associated to a transition between a shallow defect in the band gap and the valence band, see Figure 8. These levels are associated to oxygen vacancies, with simple or double ionization which is in accordance with the classification of Longo et al., (2008), vacancies bonded to clusters of TiO₅ in disordered regions. In principle, the incorporation of Nb[5+] in PZT samples would be producing more lead vacancies than oxygen vacancies. However, the higher intensities observed for peaks at 2.56 eV rather than peaks at around 1.73 eV is an indication that the oxygen vacancy concentration is higher than lead vacancies.
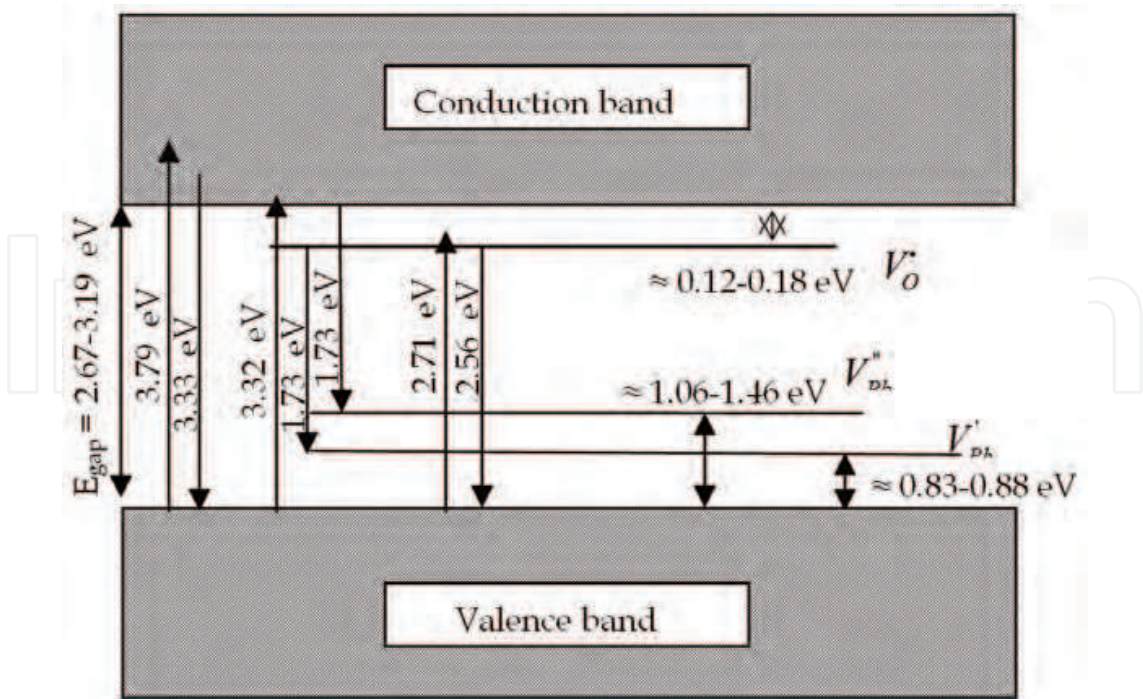

Fig. 8. Schematic diagram of recombination process associated with the emission bands in PZTN ceramics, for excitation energy 3.79, 3.31 and 2.71 eV.

2.3 Substitution in A + B site

We will present results of double substitution in place A and B for "hard" and "soft" well-known ceramic. For "hard" ceramics present $Sr^{2+} + Cr^{3+}$ doped PZT ceramics and for "soft" ceramics present $La^{3+} + Nb^{5+}$ doped PZT ceramic.

We will only present the behavior in the PZT morphotropic phase boundary region of phase diagram (Zr/Ti=53/47).

In both type of samples (hard and soft) only appear two regions of emission bands, one at around 1.86 eV and other with higher intensity at around 3.00 eV when fixing the excitation band at 373 nm (3.4 eV) (Figure 9). Also, it is possible to observe emission band around 2.5-2.7, to a lot of smaller intensity. When fixing the excitation band at 412 nm (3.01 eV) only appear one signal wide at 3.28-3.31 eV (Figure 10).

PL show in the high energy region, the maximum position is around 3.00 eV for all composition, but the emission band is a broad band composed by two bands, at 2.98eV (414nm) and 3.03eV (408 nm) (Figure 9). PL lower energy region for PSZTC and PLZTN samples show the band at 1.87 eV (659 nm), additionally is observed that band at 1.74 eV is not present in all compositions and its intensity is reduced appreciably with the incorporation of Cr (Durruthy et al, 2010a, , 2011).

The general effect of the Cr doping is a decrement the PL intensity in both region bands with the increase of dopant. It is noted that the PL of doped La^{3+} and Nb^{5+} is larger than of undoped samples and increased with the composition of both ions at least one order of magnitude for PSZTC, but is two and three order to PZTN and PLZT respectively.

It was of waiting that doped La^{3+} and Nb^{5+} increase PL intensity in 1.87 eV (659 nm) in PL, it is well known that is associated with lead vacancies, due to the compensation of charge, in this case the disorder or lead vacancy should be associated to the substitution of La^{3+} by Pb^{2+} in the host structure and the typical presence of lead vacancy due to the sintering route (Calderón-Piñar et al, 2007; Silva et al., 2005). The presence of the peak at 1.87 eV, in PSZTC 0.2-0.5 mol % and PLZTN 1 mol% indicates a common defect related with a deep level inside the band gap. As we saw in the region of high energy (3.00 eV) results are similar to showed above previously.

The peaks that appear in zone (2.65) was associated with oxygen vacancies, simple or double ionized. In the sample PLZTN evidently that E_D will be $\geq$ 0.54 eV, and E_{PL} is lower 2.43-2.74. This is because E_D is not exactly one unique value because there are a distribution defects in the structure.

The analysis of the peak at 1.86 eV could be associated to the simultaneous presence of oxygen and lead vacancies (Guiffard et al, 2005; Durruthy et al, 2010a, b, 2011). The PL response in the donor-acceptor mechanism in this case between the levels associated to the oxygen near and below conduction band and the level of lead vacancies above the valence band. Analogously the theoretical quantum mechanical calculation reported by de Lazaro et al. (2007) justify that the presence of disorder associated to the substitution of Zr/Ti or displacement of the ions in the B sites produce an amorphous zone in the ceramic with a direct band gap with a separation near to 1.87eV. Beside this, we are detecting some small peaks whose energy is around of 2.00-2.80 eV which belong to the visible energy spectra too (Figure 9).

The calculated results of the band gap values for the PSZTC samples sintered at 1250 ºC are summarized in Table 2. The figure 11 allows us to affirm that the dependence with Zr/Ti ratio is very strong, and has a maximum in the morphotropic phase boundary and the lowest values are for the composition 80/20, this behavior coincides with the calculations

carried out by J. Baedi et al. (2008). Figure 12 shows the way that would be materialize recombination in the PSZTC and PLZTN samples. We supposed that the main way was 1, 5 and 6 for the experimental results obtained, in this work.
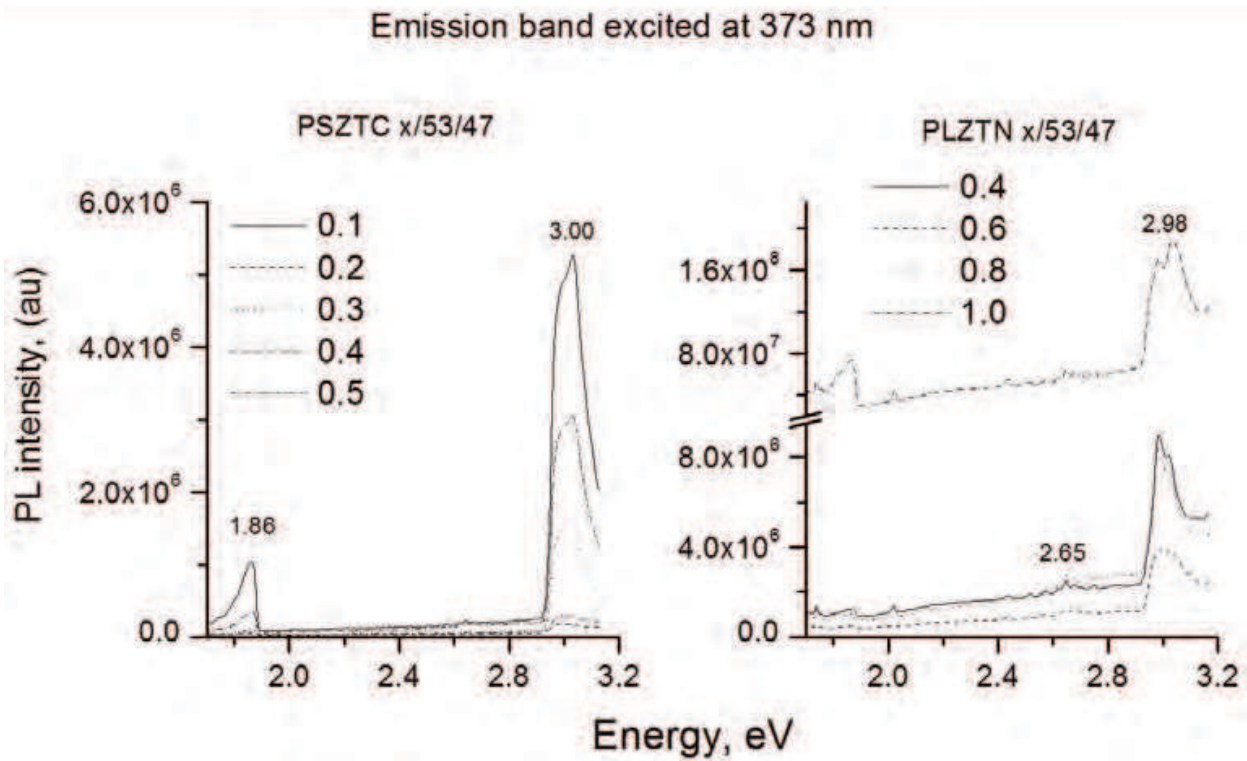

Fig. 9. Room temperature PL emission spectra for PSZTC and PLZTN ceramics at different dopant concentration, fixing exited band at 373 nm.
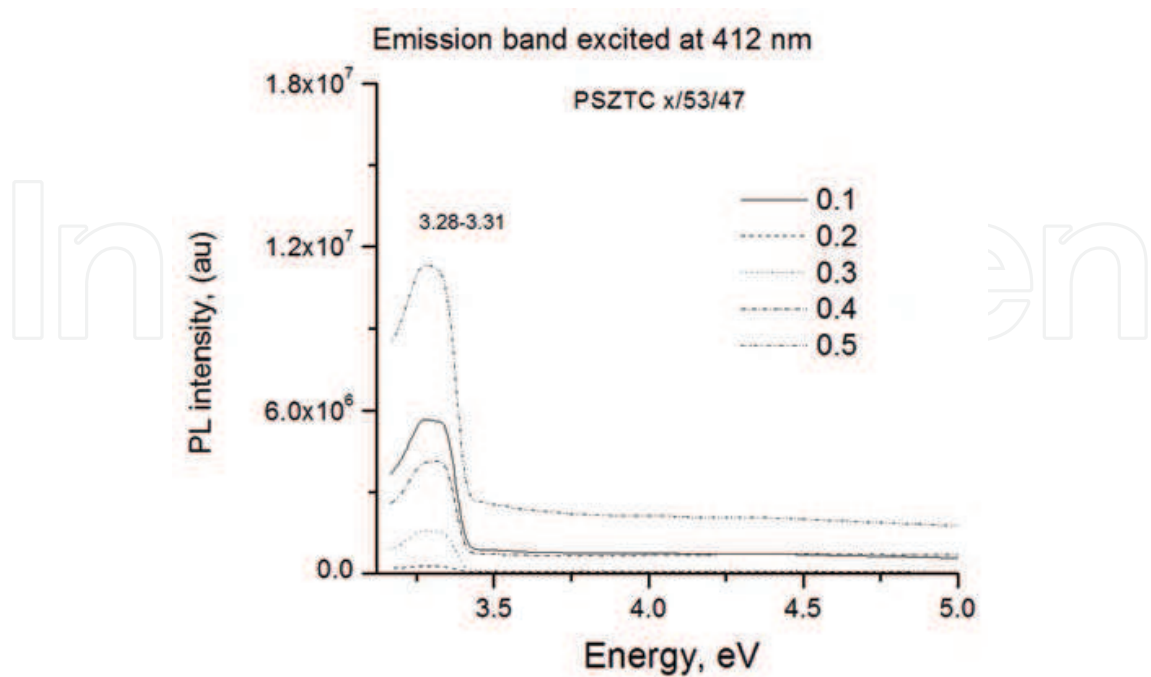

Fig. 10. PL emission spectra at room temperature for PSZTC fixing exciting at 412 nm.

PSZTC		PLZTN	
mole %	E_{gap}	mole %	E_{gap}
0.0	3.25	0.0	3.15
0.1	3.33	0.2	-
0.2	3.35	0.4	2.88
0.3	3.36	0.6	2.91
0.4	3.36	0.8	3.07
0.5	3.32	1.0	2.50

Table 2. Band gap energy (Eg) for PZT soft and hard, determined using the diffuse reflectance principle (Kubelka-Munk expression). Error Eg= ± 0.003 eV. For E_{PL} supposed E_D=0.54.
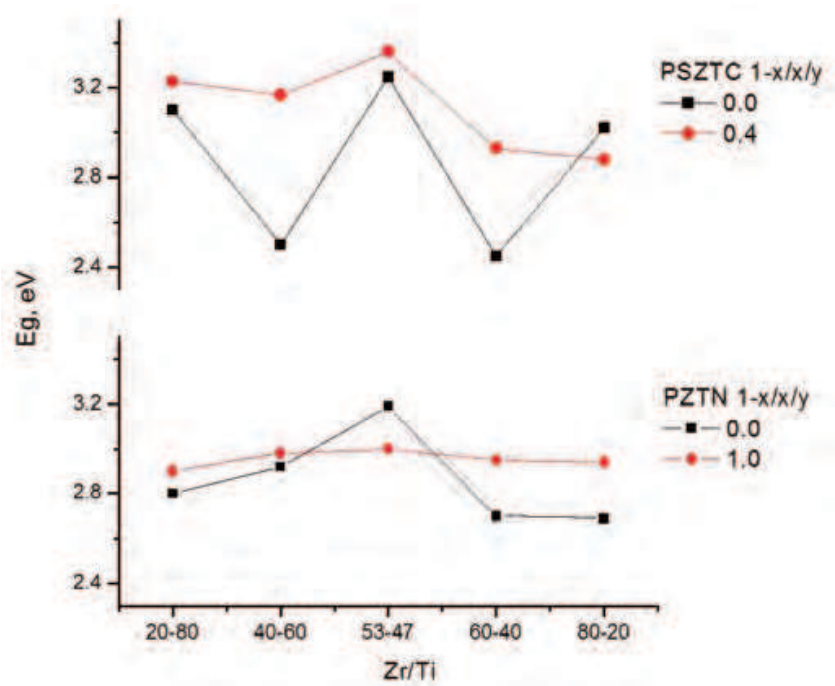

Fig. 11. Behavior of the forbidden band energy for PSZTC and PZTN ceramics, which agrees with the results obtained for J. Baedi et al. (2008)
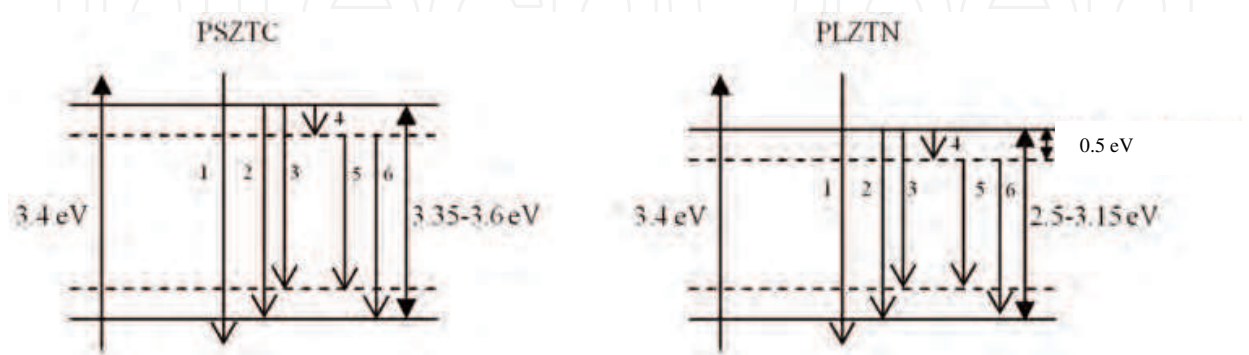

Fig. 12. Possible energetic process that will be happen in PZT ceramics. 3.4 eV is excitation energy (373 nm), 1-6 there are the possible recombination way (PL). We consider that occurred the way 1, 5 and 6 mainly.

3. Dielectric characteristic

Another characteristics of these materials that they are very affected by the presence of oxygen vacancies there are dielectric (ε) and loss (tan δ), for this we present some results in different substitution type in ABO_3 perovskite structure.

The dielectric curves reveal anomalies in the neighbor at transition temperatures corresponding to $F_{R(HT)}$ – P_C (T_C) and F_T – P_C (T_{F-P}) phase transitions. Strong influence of dopant La, Nb and La+Nb on the phase transition temperature (T_C) is confirmed. The comparison of ε(T) curves, obtained for the ceramic samples is shown in Figure 13, dielectric measurement shows a decreasing T_C and T_{F-P} when increasing the dopant concentration. The dielectric permittivity decreases for dopant concentration larger than 0.8 mol% (Figure 13), in particularity in Nb-doped ceramics permittivity decreases for concentrations up to about 0.8 mol %, and then it increases slightly, as the grain size behaves. The same as in PL, the permittivity is more intense for substitutions in B and A+B, in this case it is 4 times.

There is good agreement between the transition temperatures obtained from ε and tgδ, respectively, considering the range of measurement error (δt ~ 5 °C), for almost every sample. Those compositions with 0.6 and 1.0 % La have T tgδ_{max} at 50 kHz differing 7.3-8.2 °C from the value obtained at 1 kHz. A possible cause of such differs is the presence of inhomogeneities as a result of compositional fluctuations (Gupta & Viehland, 1998; Garcia et al., 2001).

In those samples doped with La+Nb, there is not a sum of the separate effects of La and Nb. Note that temperatures are not as low as those for Nb, but compared to those for La they are 50 °C below.
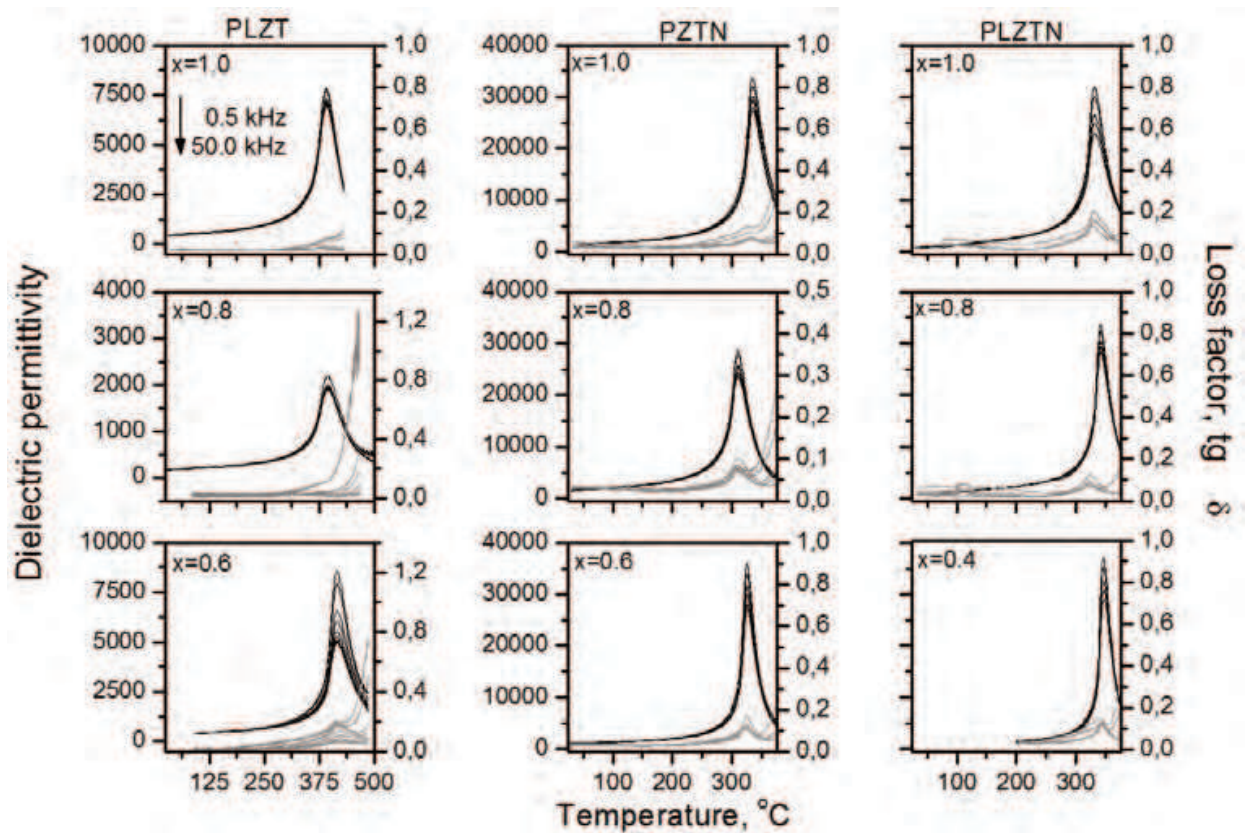

Fig. 13. Permitivity as a function of temperature, measured at various frequencies, for PZT 53/47 ceramics showing La_2O_3 , Nb_2O_5, and $Nb_2O_5+La_2O_3$ content.

Grain size decrement implies domain size decrement (Figure 14). Thus, the domain walls become more movable, so the mechanical friction is small, and then the samples doped with Nb and La+Nb are more compositionally homogenous (the evidence is given by narrow plots of dielectric permittivity vs. temperature, that is, increasing permittivity). On the other hand, grain size increment contributes to higher values of the dielectric constant, as a measurement of the number of polarized unitary cells. The amount of polarization of such cells is related to the presence of Nb^{5+} and La^{3+} inside the cristalline structure and contributes to the orientation of the domain walls. An increasing dopant concentration produces the increment of the number of lead vacancies and so the dielectric permittivity grows. The values of ε for PZTN samples are higher and attributed to the higher compositional homogeneity and the existence of only one phase in this composition. But is not the same for PLZTN and PLZT, XRD patterns of samples show the tetragonal and rhombohedral PZT phases together. (Figure 15) in all doped samples, with concentration near to MPB (53/47).

Decrements of Tc might be attributed to the integration of dopants into the cristalline structure.
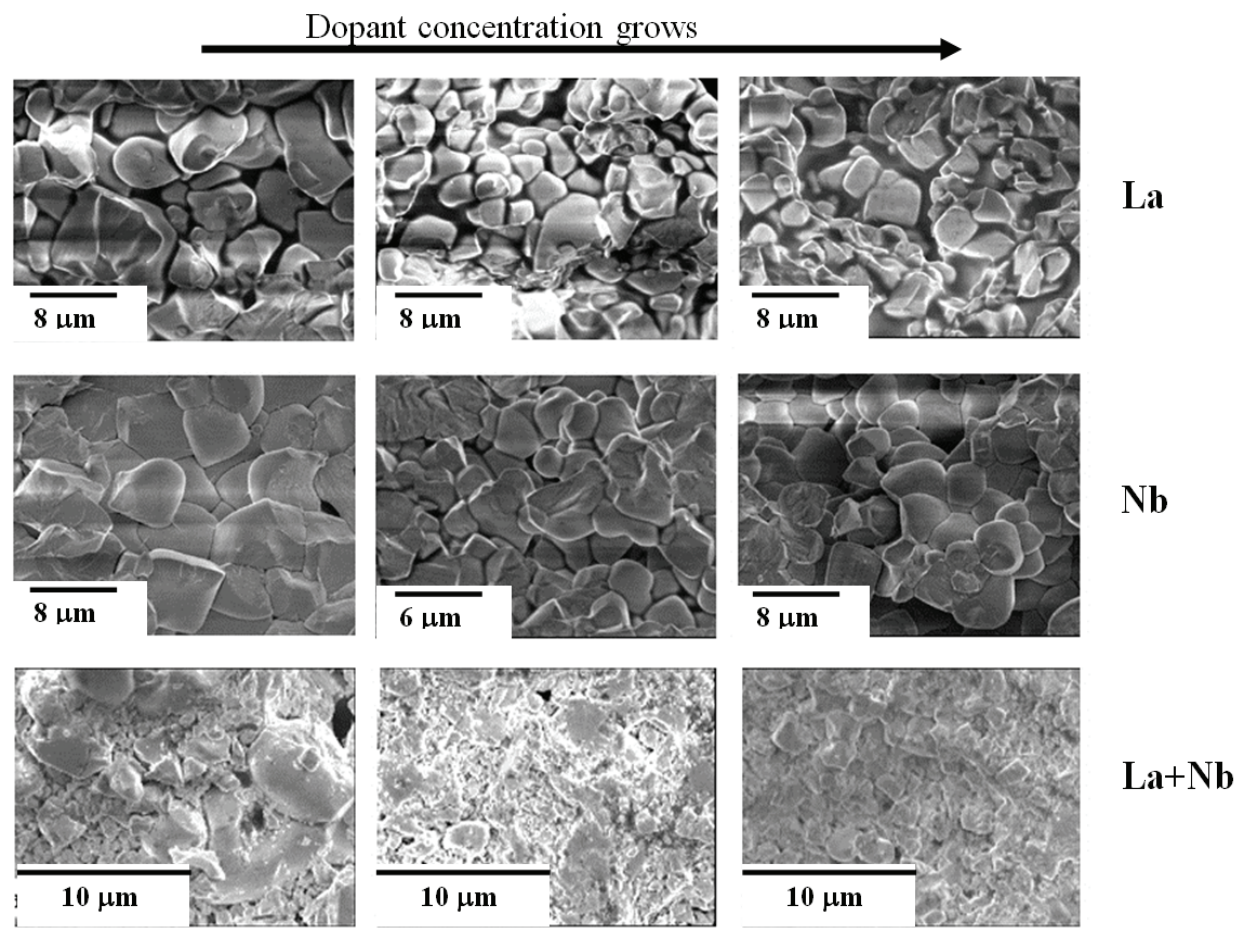

Fig. 14. SEM results for 0.6, 0.8 and 1.0 mol % dopant in study for samples near to MPB. In every case, the decrement of grain size as the dopant concentration increases is observed.
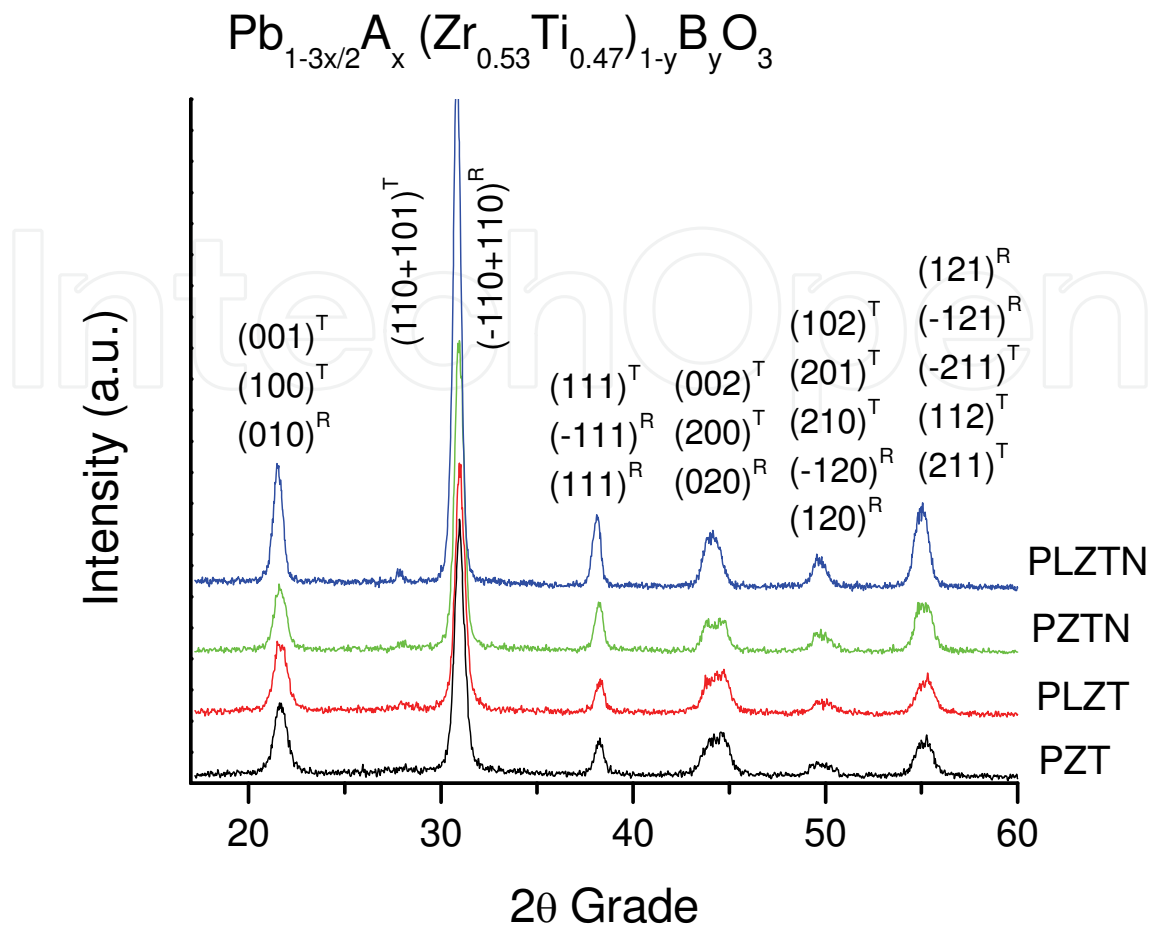
Fig. 15. Room temperature DRX patterns for PZT, PLZT, PZTN and PLZTN 53/47/1.0 sinter ceramics. Note for PZTN there are more tetragonal phase, observe better resolution of 002/200 plane.

To determine the factor most influential in dielectric permittivity behaviour with the dopant concentration, the influence of porosity was analyzed. As it was seen in Table 3 it varies in an appreciable way (~ 14%) in the studied composition interval.

Among the models proposed to evaluate the properties of porous materials, applicable to systems with inferior porosity values at 0.6, it (the model) stands out the Bruggeman model. This model offers a satisfactory description of the properties of piezoelectric porous ceramic, in particular those based on PZT. A detailed explanation can it turns in works from Wersing et al (1986).

The model establishes a peculiar relationship between experimental permittivity [$\varepsilon(p0)$] and the theoretical [$\varepsilon po=0$], through of porosity fraction ($p0$) given by the equation (5), considering connectivity (3-0).

$$\varepsilon(p_o) = \varepsilon\, p_{o=0} * (1 - p_o^{2/3}) \tag{5}$$

Table 3 shows the results for the dielectric permittivity theoretical and experimental at room temperature. A marked difference exists among both, being bigger for the Nb and the La+Nb, what indicates the influence of this impurity in the evolution of the porosity, also $\Delta\varepsilon$ to diminish with the frequency

Niobio						
Frecuencia kHz	0,2			1,0		
	$\varepsilon_{(Po)}$	$\varepsilon_{Po=0}$	$\Delta\varepsilon$	$\varepsilon_{(Po)}$	$\varepsilon_{Po=0}$	$\Delta\varepsilon$
0,5	830	1249	419	1373	1669	296
1	635	955	320	1335	1646	292
5	587	883	296	1307	1589	282
10	482	725	243	1297	1577	280
25	251	378	127	1269	1543	274
Lantano						
	0,6			1,0		
0,5	343	395	52	566	658	92
1	286	329	43	549	638	89
5	155	180	25	425	494	69
10	128	148	20	304	354	50
25	109	126	17	160	186	26
Lantano+Niobio						
	0,4			1,0		
0,5	343	588	245	784	1035	251
1	286	491	205	768	1015	247
5	155	204	49	734	970	236
10	128	220	92	710	934	224
25	109	187	78	654	864	210

Table 3. Theoretical and experimental permittivity and their difference at room temperature for 5 frequencies, for PZTN, PLZT and PLZTN 53/47/y ceramic, based on the Bruggeman model.

It is important to make notice that this model considers a materials as a not homogeneous médium and it start with two components: material and pores. In the material component there are all that is not pore, that doesn't have to be necessarily homogeneous, due to the procedure method.

The porosity is not the only factor that determines the permittivity variation with dopant concentration. The analysis for dopant type shows that to smaller concentration bigger porosity, but also bigger grain size, therefore is this last one the most influential in the variations of the dielectric parameter. For example, 0.6% of Nb, the smallest difference exists among the theoretical and experimental results, and the porosity has the fundamental rol, for this concentration "po" it is minimized; in the other concentrations exists a cooperative effect of the porosity and the grain size (Sundar et al. 1996), noted how for 1.0% "po" slightly increases the grain size and $\Delta\varepsilon$ (Table 3). In La3+ case, $\Delta\varepsilon$ diminishes with the frequency and increases with dopant concentration (Table 3), but ε is increasing with grain size decrement, therefore both factors will contribute in a cooperative way in the relative permittivity (Figure 16). The samples doped with La+Nb have a grain size between 1 and 2 microns, in

addition the contribution of the porosity is strong in the behavior of dielectric permittivity, being greater even for the composition 0.8. The factors that determined the variation of the permittivity with increasing dopant concentration are the grain size (Cancarevic et al., 2006) and porosity, fundamentally.
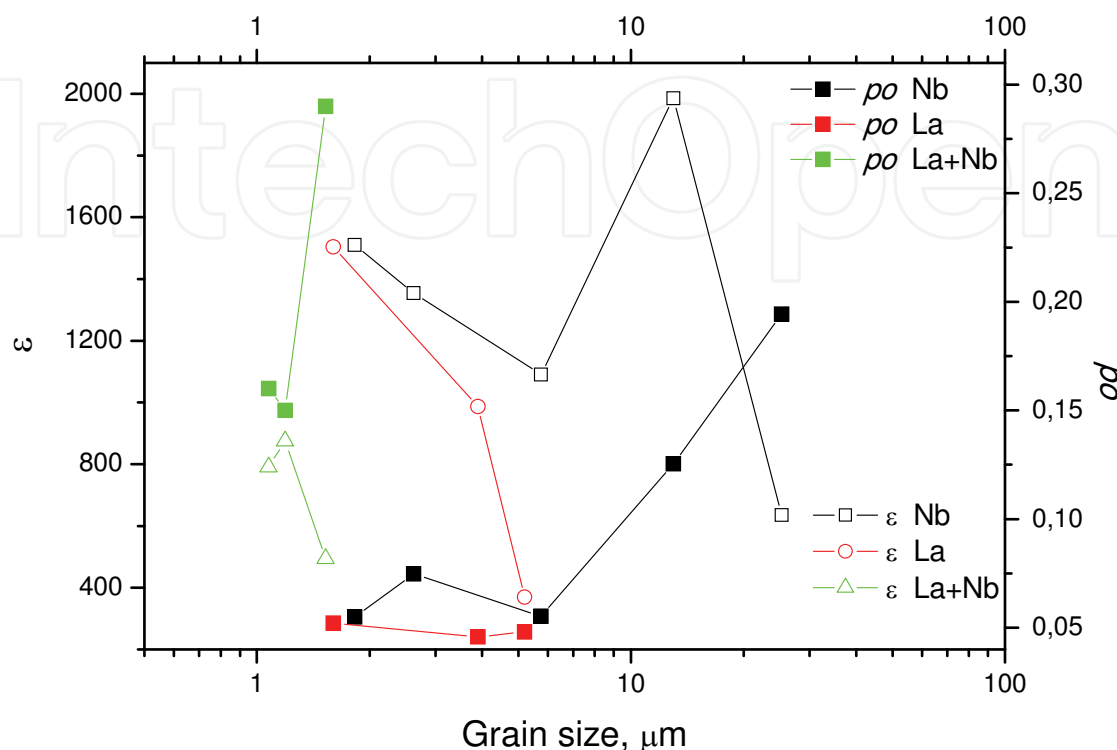

Fig. 16. Behavior at room temperature of dielectric constant (·) and porosity (po) as function of the grain size.

4. Conclusion

The used of PL and diffuse reflectance measurement in polycrystalline ceramics to determine the band gap and the mechanism of the recombination in samples is possible. The experimental results agree with those calculated.

All system present show mainly two region of emission bands around 1.8 and 3 eV, the presence of broad band (1.8 eV) at the band gap can be associated to the vacancy defect common in all (containing lead) ceramics sintered at high temperatures, the emission at around 3eV correspond to direct recombination from CB to VB .

The emission at 2.56 eV, this present but it is not very intense in all the analyzed materials. Shows the highest intensity and a shift to higher energies in the tetragonal phases. The Nb concentration produces appreciably intensity changes and is associated to a transition from oxygen vacancy levels to valence band. PZTN presents the biggest intensity in this band, what indicates that the oxygen vacancy concentration is higher than lead vacancies.

But not all the dopant has same behavior, in all zone of PL spectra Cr diminish PL intensity with increase concentration, while La^{3+}, Nb^{5+} and $La^{3+}+Nb^{5+}$ increase PL intensity with the increase dopant concentration.

Another interesting aspect is that A+B doped produces an increment to 2-3 order in PL intensity, principally for "soft" doped.

On the other hand, a strong influence of dopants on the decrement of grain size as concentration grows is observed. The substitution in the A place and the simultaneous substitutions in the A and B places provokes mixture of (tetragonal and rombohedral) phases, while substitution in the B place the structure is tetragonal at least in 95 %. A texture effect is also noticed, as it grows with the dopant concentration.

XRD results are confirmed by the obtained dielectric characteristics. In the PLZT, PLZTN and PSZTC samples which present phase mixture, two peaks in the $1/\varepsilon$ curves are observed and associated to Ferro-Ferro (rombohedral-tetragonal) and Ferro-Para (tetragonal-cubic) phase transitions. Substitutions in the B place contribute more significantly to the Curie temperature drop, with a minimum for PZTN 0.8 %.
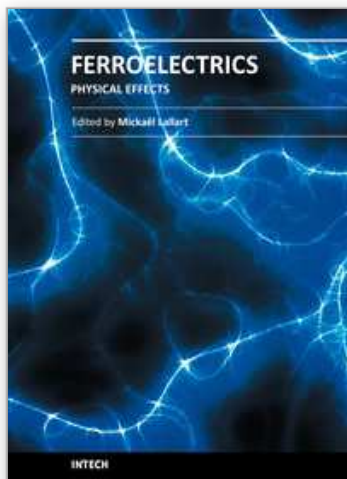
5. Acknowledgements

6. Reference

Anicete-Santosa, M., Silva, M.S., Orhan, E., Gomes, M. S., Zaghete, M. A., Paiva-Santos, C. O., Pizani, P. S., Cilense, M., Varela, J. A., Longo, E., (2007) Contribution of structural order–disorder to the room-temperature photoluminescence of lead zirconate titanate powders. Journal of Luminescence, Vol. 127, Issue 2, 689-695

Baedi, J., Hosseini, S.M., Kompany, A., (2008) The effect of excess titanium and crystal symmetry on electronic properties of Pb(Zr1?xTix)O3 compounds. Computational Materials Science, Vol: 43, Issue: 4, 909-916, ISSN: 09270256.

Bharadwaja, S.S.N., Saha, S., Bhattacharyya, S., Krupanidhi, S.B., (2002) Dielectric properties of La-modified antiferroelectric PbZrO 3 thin films. Materials Science and Engineering B vol 88, issue 1, 22-25, ISSN 0921-5107

Calderón-Piñar, F., Aguilar, J., García, O., Fuentes, J., Contreras, G., Durruthy-Rodríguez, M. D., Peláiz-Barranco, A., (2007) Mediciones de fotoluminiscencia en sistema PLZT para determinar su relación con los mecanismos de conducción. Mediciones térmicas de materiales sinterizados tipo BSZT. Instituto de Cibernética, Matemática y Física (I CIMAF) Research Report 2007-412, ISSN 0138-8916

Cancarevic, M., Zinkeivich, M., Aldinger, F., (2006) Thermodynamic Assessment Of The Pzt System Journal Of The Ceramic Society Of Japan, Vol. 114, Issue:1335, 937-949, ISSN 0914-5400

Chang, Q. Sun, Jin, D., Zhou, J., Li, S., Tay, B.K., Lau, S.P., Sun, X.W., Huang, H.T., Hing, P., (2001) *Intense and stable blue-light emission of Pb($Zr_x Ti_{1-x}$)O₃.* Applied Physics Letters Vol 79, No. 6, 1082-1084, ISSN 1077-3118

Chen, J., Chan, H.M., Harmer, M., (1989) Ordering Structure and Dielectric Properties of Undoped and La/Na-doped Pb(Mg1/3Nb2/3)O3. J. Am. Ceram. Soc. Vol. 72, No. 4, 593-598, ISSN 0002-7820

de Lazaro, S., Milanez, J., de Figueiredo, A.T., Longo. V.M., Mastelaro,V.R., de Vicente, F.S., Hernandes, A.C., Varela, J.A., Longo E., (2007) Relation between

photoluminescence emission and local order-disorder in the CaTiO3 lattice modifier. Applied Physics Letters 90, 111904-1 - 111904-3, ISSN 0003-6951

Dixit, A., Majumder, S. B., Katiyar, R. S., Bhalla, A. S., (2006) Studies on the Relaxor Behavior of Sol-Gel Derived Ba(ZrxTi1-x)O3 (0.30 ≤ x ≤ 0.70) Thin Films. Journal of Materials Science 41, 87, ISSN 0022-2461

Durruthy, M. D., Fuentes, L., Hernandez, M., Camacho , H. (1999) Influence of the niobium dopant concentration on the Pb(Zr0.54Ti0.46)O3 ceramics sintering and final properties. Journal of Materials Science 34 2311 – 2317

Durruthy-Rodríguez, M.D., Hernández-García, M., Suárez- Gómez A. (2002) Lanthanum and niobium doping on PZT ceramic synthesis. Revista CENIC Ciencias Químicas, Vol. 33, No. 1, 29-33, ISSN 0254-0525

Durruthy-Rodríguez, M.D., Costa-Marrero, J., Hernández-García, M., Calderón-Piñar, F., Yañez-Limón, J.M. (2010a) Photoluminescence in "hard" and "soft" ferroelectric ceramics. Applied Physics A, 98, 543–550, DOI 10.1007/s00339-009-5501-y

Durruthy-Rodríguez, M. D., Costa-Marrero, J., Hernández-Garcia, M., Calderón-Piñar, F., Malfatti, C., Yañez-Limón, J. M., Guerra, J. D. S. (2010b) Optical characterization in $Pb(Zr_{1-x}Ti_x)_{1-y}Nb_yO_3$ ferroelectric ceramic system. Applied Physics A, DOI 10.1007/s00339-010-6017-1, ISSN 1432-0630

Durruthy-Rodríguez, M.D., Costa-Marrero, Calderón-Piñar, F., Yañez-Limón, J.M., Guerra , J. D. S., (2011) Photoluminescence in Pb0.95Sr0.05(Zr1-xTix)1-yCryO3 ferroelectric ceramic system. Journal of Luminiscence (accepted), ISSN 0022-2313

Eyraud, L., Guiffard, B., Lebrun, L., Guyomar, D., (2006) Interpretation of the Softening Effect in PZT Ceramics Near the Morphotropic Phase Boundary. Ferroelectrics Vol. 330, issue 1, 51-60, ISSN 0015-0193

Garcia, S., Font, R., Portelles, J., Quiñones, R.J., Heiras, J., Siqueiros, J.M. (2001) Effect of Nb doping on (Sr,Ba) TiO3 (BST) ceramic samples. Journal of Electroceramics, Vol. 6, No. 2, 101-108, ISSN 1385-3449

Ghasemifard M., Hosseini S.M., Khorsand Zak A., Khorrami Gh. H. (2009) Microstructural and optical characterization of PZT nanopowder prepared at low temperature. Physica E: Low-dimensional Systems and Nanostructures, Volume 41, Issue 3, 418-422, ISSN 13869477

Guiffard, B., Boucher, E., Eyraud, L., Lebrun, L., Guyomar, D., (2005) Influence of donor co-doping by niobium or fluorine on the conductivity of Mn doped and Mg doped PZT ceramics. Journal of the European Ceramic Society, Volume 25, Issue 12, 2487-2490, ISSN 0955-2219

Gupta, S.M., Viehland, D., (1998) Tetragonal to rhombohedric transformation in the lead zirconium titanate lead magnesium niobate-lead titanate crystalline solution. J. Appl. Phys., 83, 1407-414. ISSN 1089-7550

Haertling, G. H. Ferroelectric (1999) Ceramics: History and Technology. Journal of the American Ceramic Society, Vol. 82, 4, 797–818, DOI:10.1111/j.1151-2916.1999.tb01840.x

Jaffe, B., Roth, R.S., Marzullo, S. (1954) Piezoelectric Properties of Lead Zirconate-Lead Titanate Solid-Solution Ceramics. Journal of Applied Physics, Volume 25, Issue 6, 809-810, ISSN 0021-8979

Jaffe, B.; Cook, W.R; Jaffe, H., (1971) Piezoelectric Ceramics, Academic Press, London and New York, ISBN 0-. 12-379550-8

Kottim G. (1969) Reflectance Spectroscopy, Springer Verlag, New York. ISBN 0 19 850778x

Lines, M. E., Glass, A. M., (2001) Principles and applications of ferroelectrics and related materials, Oxford University Press Inc., New York.

Longo V. M., Cavalcante L. S., de Figueiredo A. T., Santos L. P. S., Longo E., Varela J. A., Sambrano J. R., Paskocimas C. A., De Vicente F. S. and Hernandes A. C. (2007) Highly intense violet-blue light emission at room temperature in structurally disordered SrZrO3 powders. Applied Physics Letters 90, 091906-1 - 091906-3. ISSN: 0003-6951

Longo, E., de Figueiredo, A.T., Silva, M.S., Longo, V.M., Mastelaro, V.R., Vieira, N.D., Cilense, M., Franco, R.W.A., Varela, J.A., (2008) Influence of Structural Disorder on the Photoluminescence Emission of PZT Powders. J. Phys Chem A. 112, 8953-8957, ISSN 1089-5639

Mansimenko Y.L., Glinchuk M.D., Bykov I.P. (1998) Photoinduced Centers in the Optically Transparent PLZT(8/65/35) Ceramics. Jounal of the Korean Physical Society 32, S1039-S1041, ISSN 0038-1098

Nakajima H., Mori, T., Itoh, S., Watanabe, M., (2004) Photoluminescence properties of trace amounts of Pr and Tb in yttria-stabilized zirconia. Solid State Communications vol. 129, issue 7, 421-424

Noheda, B., Cox, D.E., Shirane, G., Guo, R., Jones, B., Cross, L.E., (2001) Stability of the monoclinic phase in the ferroelectric perovskite $Pb(Zr_{1-x}Ti_x)O_3$. Physical Review B (Condensed Matter) 63, 014103-1, 1550-235X

Noheda, B., Gonzalo, J.A., Cross, L.E., Guo, R., Park, S.E., Cox, D.E., Shirane, G., (2000)Tetragonal-to-monoclinic phase transition in a ferroelectric perovskite: The structure of $Pb(Zr_{0.52}Ti_{0.48})O_3$. Physical Review B 61, 8687-8695, DOI:10.1103/PhysRevB.61.8687

Ronda C. (2008) Luminescence: From Theory to Applications. Edited by WILEY-VCH Verlag GmbH & Co. KGaA, ISBN: 978-3-527-31402-7, Weinheim.

Shannigrahi, S.R., Tripathy, S. (2007) Micro-Raman spectroscopic investigation of rare earth-modified lead zirconate titanate ceramics. Ceramics International vol. 33, n 4, 595-600, ISSN 0272-8842

Silva, M.S., Cilense, M., Orhan, E., Gomes, M.S., Machado, M.A.C., Santos, L.P.S., Paiva-Santos, C.O., Longo, E., Varela, J.A , Zaghete, M.A., Pizani, P.S., (2005)The nature of the photoluminescence in amorphized PZT. Journal of Luminescence 111, 205–213, DOI:10.1016/j.jlumin.2004.08.045

Sivasubramanian V., Kesavamoorthy R., Subramanian V. (2007) Photoluminescence investigations on the nanoscale phase transition in Pb(Mg1/3Nb2/3)O3. Solid State Communications Vol. 142, Issue 11, 651-654, ISSN 0038-1098

Suárez-Gómez, A., Durruthy, M. D., Costa-Marrero, J., Peláiz-Barranco, A., Calderón-Piñar, F., Saniger-Blesa, J. M., de Frutos, J.(2009) Properties of the PLZTN x/54/46 (0.4 ≤ x ≤ 1.4) ceramic system. Materials Research Bulletin vol. 44, 1116–1121, ISSN 0025-5408

Sundar, V., Kim, N., Randall, C.A., Yimnirun, R., Newnham, R.E. (1996) The effect of Doping and grain size on Electrostriction in PbZr0.52 Ti0.48O3. IEEE, 1, 935-938, ISBN 0-7803-3355-1

Tai, C.W. & Baba-Kishi, K.Z. (2002) *Microtexture studies of PST and PZT ceramics and PZT thin film by electron backscatter diffraction patterns.* Textures and Microstructures, Vol. 35, No. 2, 71–86, ISSN 1029-4961.

Wendlandt, W.W., Hecht, H.G (1966) Reflectance Spectroscopy, Wiley Interscience, New York, BCIN Number 62796

Wersing W., Lubitz K., Mohaupt J. (1986) Dielectric, elastic and piezoelectric properties of porous PZT ceramics. Ferroelectrics, 68, 77-79. ISSN 0015-0193

Yang, Z., Liu, Q.-H., (2008) The structural and optical properties of ZnO nanorods via citric acid-assisted annealing route. Journal of Materials Science, Volume 43, Number 19, 6527-6530, ISSN 0022-2461

Yu, P.Y., Cardona, M., (1996) Fundamentals of semiconductors. Physics and Materials Properties. Ed. Springer-Verlag, Berlin, ISBN 978-3-642-00710-1

Ferroelectrics - Physical Effects

Edited by Dr. Mickaël Lallart

Ferroelectric materials have been and still are widely used in many applications, that have moved from sonar towards breakthrough technologies such as memories or optical devices. This book is a part of a four volume collection (covering material aspects, physical effects, characterization and modeling, and applications) and focuses on the underlying mechanisms of ferroelectric materials, including general ferroelectric effect, piezoelectricity, optical properties, and multiferroic and magnetoelectric devices. The aim of this book is to provide an up-to-date review of recent scientific findings and recent advances in the field of ferroelectric systems, allowing a deep understanding of the physical aspect of ferroelectricity.

How to reference

In order to correctly reference this scholarly work, feel free to copy and paste the following:

M. D. Durruthy-Rodríguez and J. M. Yáñez-Limón (2011). Photoluminescence in Doped PZT Ferroelectric Ceramic System, Ferroelectrics - Physical Effects, Dr. Mickaël Lallart (Ed.), ISBN: 978-953-307-453-5, InTech, Available from: http://www.intechopen.com/books/ferroelectrics-physical-effects/photoluminescence-in-doped-pzt-ferroelectric-ceramic-system

INTECH
open science | open minds